

# The imprint of the cosmic supermassive black hole growth history on the 21 cm background radiation

Takamitsu L. Tanaka<sup>1,2\*</sup>, Ryan M. O’Leary<sup>3</sup>, Rosalba Perna<sup>1,3</sup>

<sup>1</sup>*Department of Physics and Astronomy, Stony Brook University, Stony Brook, NY 11794, USA*

<sup>2</sup>*Department of Physics, New York University, 4 Washington Place, New York, NY 10003, USA*

<sup>3</sup>*JILA, University of Colorado and NIST, 440 UCB, Boulder, CO 80309-0440, USA*

## ABSTRACT

The redshifted 21 cm transition line of hydrogen tracks the thermal evolution of the neutral intergalactic medium (IGM) at “cosmic dawn,” during the emergence of the first luminous astrophysical objects ( $\sim 100$  Myr after the Big Bang) but before these objects ionized the IGM ( $\sim 400 - 800$  Myr after the Big Bang). Because X-rays, in particular, are likely to be the chief energy courier for heating the IGM, measurements of the 21 cm signature can be used to infer knowledge about the first astrophysical X-ray sources. Using analytic arguments and a numerical population synthesis algorithm, we argue that the progenitors of supermassive black holes (SMBHs) should be the dominant source of hard astrophysical X-rays—and thus the primary driver of IGM heating and the 21 cm signature—at redshifts  $z \gtrsim 20$ , if (i) they grow readily from the remnants of Population III stars and (ii) produce X-rays in quantities comparable to what is observed from active galactic nuclei and high-mass X-ray binaries. We show that models satisfying these assumptions dominate over contributions to IGM heating from stellar populations, and cause the 21 cm brightness temperature to rise at  $z \gtrsim 20$ . An absence of such a signature in the forthcoming observational data would imply that SMBH formation occurred later (e.g. via so-called direct collapse scenarios), that it was not a common occurrence in early galaxies and protogalaxies, or that it produced far fewer X-rays than empirical trends at lower redshifts, either due to intrinsic dimness (radiative inefficiency) or Compton-thick obscuration close to the source.

**Key words:** cosmology: theory, cosmology: dark ages, reionization, first stars, quasars: supermassive black holes, intergalactic medium

## 1 INTRODUCTION

Supermassive black holes (SMBHs) reside in the hearts of most massive galaxies (see Kormendy & Ho 2013 for a review). Through luminous quasar episodes, they may play key roles in shaping their galactic and intergalactic environments (e.g. Ricotti & Ostriker 2004; Cattaneo et al. 2009). Discoveries of quasars at redshifts  $z \sim 6 - 7$  have revealed that SMBHs with masses of several  $10^9 M_\odot$  were already in place when the Universe was less than a Gyr old (e.g. Fan et al. 2001; Willott, McLure & Jarvis 2003; Willott et al. 2010; Mortlock et al. 2011; Venemans et al. 2013).

Despite the astrophysical significance of SMBHs and their presence throughout cosmic time, their origins are not well constrained by current observations and remain a subject of active investigation (see reviews by Volonteri 2010; Haiman 2013).

Broadly speaking, theoretical hypotheses of “seed” BHs that grow into SMBHs fall into one of two categories. The first type of seeds are remnants of the earliest stars (Population III, or PopIII, stars), which form with masses  $\sim 10 - 100 M_\odot$  at redshifts  $z \gtrsim 20$  (Abel, Bryan & Norman 2002; Bromm, Coppi & Larson 2002; Yoshida, Omukai & Hernquist 2008; Stacy, Greif & Bromm 2010; Greif et al. 2011; Hirano et al. 2014), and subsequently grow through a combination of gas accretion and mergers (e.g., Haiman & Loeb 2001, Madau & Rees 2001; additional references in the detailed description in §2). The second class of seeds, called “direct collapse” BHs (DCBHs hereafter), forms with much greater initial masses,  $\sim 10^4 - 10^5 M_\odot$  at later times  $z \lesssim 15$ . They form inside gas clouds that do not fragment to form ordinary stars, but instead collapse to form a much more massive compact object (e.g. Bromm & Loeb 2003, Koushiappas, Bullock & Dekel 2004, Begelman, Volonteri & Rees 2006, Lodato & Natarajan

\* E-mail: takamitsu.tanaka@stonybrook.edu

2006). Both families of seed models require the seed BHs to grow at rates comparable to the Eddington rate to explain the observed  $\sim 10^9 M_\odot$  quasar SMBHs at  $z \approx 6 - 7$ , with an average  $e$ -folding timescale no longer than  $40 - 50$  Myr between seed formation and  $z \approx 7$  (e.g. Tanaka 2014).

Currently, there are few observational constraints on the cosmic history of SMBHs at  $z > 6$ . The  $z \sim 6$  quasar luminosity function and inferred underlying SMBH mass function leaves many degrees of freedom for theoretical explanations. The main empirical constraints are that models should grow enough  $\sim 10^8 - 10^9 M_\odot$  SMBHs to account for the quasar observations, and that they exceed neither empirical estimates of the universal SMBH mass density nor the unresolved cosmic X-ray background (e.g. Tanaka & Haiman 2009; Salvaterra et al. 2012). There is no firm empirical evidence that favors either kind of seed model, places meaningful constraints on how common the seeds were, or indicates whether they grew steadily (e.g., spurred by the frequency of major galaxy mergers at these large redshifts Li et al. 2007; Tanaka 2014) or in shorter, intermittent spurts<sup>1</sup> (Volonteri & Rees 2005; Madau, Haardt & Dotti 2014; Volonteri, Silk & Dubus 2015). Even future direct observations of quasars at  $z \gtrsim 7$  may not be able to distinguish between the PopIII and DCBH seed scenarios—most published SMBH growth models for both scenarios are consistent with the existence of  $\sim 10^5 M_\odot$  SMBHs at  $z \sim 12$  (a condition that comes about naturally if the progenitors of the  $z \sim 6 - 7$ ,  $\sim 10^9 M_\odot$  quasar SMBHs grew at near the Eddington limit).

In this work, we show that upcoming observations of the sky-averaged redshifted 21 cm line from the hyperfine transition of neutral hydrogen can help elucidate the growth history and abundance of SMBHs at  $z \gtrsim 20$  (Ricotti, Ostriker & Gnedin 2005; Ripamonti, Mapelli & Zaroubi 2008; Mirocha, Harker & Burns 2013). This line appears in absorption if the gas spin temperature is lower than that of the cosmic microwave background (CMB), and in emission otherwise; it can thus be used to map the thermal history of the intergalactic medium prior to cosmic reionization (see Furlanetto, Oh & Briggs 2006 for a review). The strength of the 21 cm transition is particularly sensitive to the thermal state of the gas, due to the coupling of the spin temperature with the gas temperature via collisions and the Lyman- $\alpha$  background (Wouthuysen 1952; Field 1958). Astrophysical sources at “cosmic dawn,” prior to cosmic reionization ( $z \gtrsim 11$ ), leave an imprint in this line by building up a Lyman- $\alpha$  background and by heating and ionizing the IGM (see, e.g., Furlanetto 2006; Pritchard & Loeb 2008; Mirocha, Harker & Burns 2013; Yajima & Khochfar 2014).

X-rays can contribute strongly to this signature because they can raise the IGM spin temperature to above the CMB temperature before fully reionizing it (Ricotti & Ostriker 2004). The imprint should be seen in the sky-averaged (global) signature, because the long mean-free path of X-rays (with energies  $\gtrsim 1$  keV) allows them to heat the

IGM nearly isotropically. The two strongest classes of X-ray sources at cosmic dawn are expected to be seed BHs accreting gas en route to growing into SMBHs and high-mass X-ray binaries (HMXBs).

In this paper, we argue that if the SMBHs observed as quasars at  $z \sim 6$  grew from PopIII seeds via radiatively efficient gas accretion, they should leave a strong increase in the 21 cm brightness temperature at  $z \gtrsim 20$ . The absence of this feature in future observations would imply either that most SMBHs formed at later epochs, that their growth was rare, or that they produce much less energy in X-rays relative to their mass growth than the standard accretion-disc interpretation of luminous AGN activity.

This paper is organized as follows. In §2, we present a series of analytic estimates to show that, for a wide range of assumptions, the X-ray output due to SMBH growth at  $z \gtrsim 6$  dominates over that associated with HMXB activity. §3 presents the physical and numerical implementation of the PopIII and the DC models for the growth of the SMBHs, and the corresponding heating history of the IGM in the two scenarios. The computation of the 21 cm signal is presented in §3.1, together with the contribution from stars. We summarize our main results and conclude in §5.

## 2 ANALYTIC ESTIMATES OF X-RAY OUTPUTS

In this section, we compare the X-ray output from two classes of astrophysical sources—accreting nuclear BHs in the earliest haloes (galaxies), and HMXBs.

### 2.1 Estimates of total emitted X-ray energy densities

The comoving SMBH mass density in the local Universe is  $\rho_{\text{SMBH}}(z=0) \sim 4 \times 10^5 M_\odot \text{Mpc}^{-3}$  (e.g. Aller & Richstone 2002; Yu & Tremaine 2002; Marconi et al. 2004; Shankar et al. 2004). Linking AGN luminosity functions with SMBH mass growth via Soltan’s argument (Soltan 1982), the same quantity at  $z \sim 6$  is estimated to be  $\rho_{\text{SMBH}}(z \approx 6) \gtrsim 10^4 M_\odot \text{Mpc}^{-3}$ , i.e. ninety per cent is thought to have been accumulated at a radiative efficiency  $\eta \equiv L/(\dot{M}c^2) \sim 0.07$  via gas accretion since  $z \sim 6$  (Shankar, Weinberg & Miralda-Escudé 2009; Shankar et al. 2010). On average, AGN emit a fraction  $f_{\text{bol}} \sim 0.05$  of their total light in  $2 - 10$  keV X-rays (e.g. Hopkins, Richards & Hernquist 2007, and refs. therein); accreting stellar-mass BHs and IMBH candidates emit the bulk of their light in X-rays (e.g. Fender & Belloni 2012), a property that’s consistent with the standard theory of luminous accretion discs (Shakura & Sunyaev 1973), which predicts that lower-mass BHs have harder accretion spectra at the same Eddington fraction.

Therefore, if the precursors to SMBHs grew via the same accretion mode as in the standard picture for luminous AGN at lower redshifts, the total comoving X-ray energy density they would have emitted prior to  $z \sim 6$  can be

<sup>1</sup> Observations do indicate that the duty cycle of quasars increases to  $\gtrsim 50\%$  at  $z > 4$ , compared to  $\lesssim 1\%$  at  $z < 2$ —see, e.g., refs.—suggesting that SMBH growth is not very intermittent, at least at  $4 \lesssim z < \lesssim$ .

estimated as

$$\epsilon_{\text{BH},X}(z > 6) \lesssim \eta f_{\text{bol}} \rho_{\text{SMBH}}(z \approx 6) c^2 \\ \sim 100 \left( \frac{\eta_{\text{BH}}}{0.07} \right) \left( \frac{f_{\text{bol}}}{0.05} \right) M_{\odot} c^2 \text{ Mpc}^{-3}. \quad (1)$$

Observations show that in the absence of X-ray AGN activity, star-forming galaxies at low redshift produce, on average, 2 – 10 keV X-ray luminosities proportional to their star formation rate  $\dot{M}_*$ , with

$$L_{*,X} \sim \ell_X \dot{M}_*, \quad (2)$$

where  $\ell_X \gtrsim 10^{39} \text{ erg s}^{-1} M_{\odot}^{-1} \text{ yr}$  (Grimm, Gilfanov & Sunyaev 2003; Basu-Zych et al. 2013; Mineo, Gilfanov & Sunyaev 2012; Mineo et al. 2014) is the factor of proportionality. Most of the X-ray luminosity is attributable to HMXB activity, which tracks young stellar populations. The above relationship can also be expressed as a radiative efficiency (i.e. the 2 – 10 keV energy emitted as a fraction of the rest mass energy of stars formed):

$$\eta_{*,X} \equiv \frac{L_{*,X}}{\dot{M}_* c^2} = \ell_X c^{-2} \approx 1.8 \times 10^{-8} \ell_{X,39}, \quad (3)$$

where  $\ell_{X,39}$  is  $\ell_X$  in units of  $10^{39} \text{ erg s}^{-1} M_{\odot}^{-1} \text{ yr}$ .

If dark matter haloes with virial temperatures  $T_{\text{vir}} > 10^4 \text{ K}$  (in the atomic hydrogen cooling regime) undergo rapid star formation, and convert  $f_* \sim 10\%$  of their baryonic mass to stars (e.g. Fukugita & Peebles 2004), then the total luminosity density of hard X-rays emitted by star-forming galaxies prior to  $z \sim 6$  is

$$\epsilon_{*,X}(z > 6) \sim \eta_{*,X} f_* \frac{\Omega_b}{\Omega_0} \rho_{\text{halo}}(M > M_4; z = 6) \\ \sim 0.8 \ell_{X,39} \left( \frac{f_*}{0.1} \right) M_{\odot} c^2 \text{ Mpc}^{-3}. \quad (4)$$

Above,  $M_4 \equiv M(T_{\text{vir}} = 10^4 \text{ K})$  is the atomic-cooling halo mass threshold,  $\Omega_b/\Omega_0 \approx 0.15$  is the ratio of the baryonic fraction to the matter fraction and  $\rho_{\text{halo}}(M > M_4; z = 6) \approx 3 \times 10^9 M_{\odot} \text{ Mpc}^{-3}$  is the  $z \sim 6$  comoving mass density locked inside dark matter haloes above this threshold (computed using the Sheth-Tormen mass function, Sheth & Tormen 2002). Note that this estimate for  $\epsilon_{*,X}$  is dominated by stars in low-mass haloes just above the atomic-cooling threshold  $M_4$ .

The ratio of total X-ray energy density emitted by SMBH progenitors to that emitted by HMXBs is then

$$\frac{\epsilon_{\text{BH},X}(z > 6)}{\epsilon_{*,X}(z > 6)} \sim 100 \left( \frac{\eta_{\text{BH}}}{0.07} \right) \left( \frac{f_{\text{bol}}}{0.05} \right) \ell_{X,39}^{-1} \left( \frac{f_*}{0.1} \right)^{-1}. \quad (5)$$

It's plausible that the earliest galaxies emitted more X-rays per unit mass of star formation—i.e. that they had more prolific HMXB activity and thus a systematically higher value of  $\ell_X$ . Basu-Zych et al. (2013) concluded that this quantity is consistent with rising as  $\propto (1+z)$  out to  $z \approx 4$ . Using the unresolved cosmic X-ray background as a constraint, Dijkstra et al. (2012) ruled out  $\ell_X(z)$  that rises more steeply than a power-law  $\propto (1+z)$  for  $\ell_{X,39}(z=0) = 3$ . Several studies (Fragos et al. 2013a,b; Hummel et al. 2014; Ryu, Tanaka & Perna, R 2015) have suggested that  $\ell_X$  may be a factor  $\sim 1-100$  higher than what is observed in lower- $z$  galaxies. Even accounting for the possibility of higher  $\ell_X$  for the earliest stellar populations, equation (5) suggests that

$\epsilon_{\text{BH},X}(z > 6) \gg \epsilon_{*,X}(z > 6)$ —at  $z > 6$ , and that total X-ray production from SMBH growth should have dominated over that from stellar populations.

We should also note that the above estimates for the SMBH mass density only account for the massive nuclear BHs identified in low-redshift observations. For example, it is possible that intermediate-mass ( $< 10^5 M_{\odot}$ ) reside in the outskirts of massive galaxies (e.g. Islam, Taylor & Silk 2003; O'Leary & Loeb 2009; Micic, Holley-Bockelmann & Sigurdsson 2011; Rashkov & Madau 2014) or in the nuclei of dwarf galaxies (e.g. Ho et al. 1997; Izotov & Thuan 2008; Barth et al. 2004; Reines, Greene & Geha 2013). The expressions above do not account for the  $z > 6$  X-ray emission from the growth of such BHs.

Note that the above estimate applies to both PopIII and DCBH seed scenarios, as long as they arrive at the  $z \approx 6$  comoving SMBH mass density of  $\sim 10^4 M_{\odot} \text{ Mpc}^{-3}$  via luminous gas accretion.

## 2.2 Estimates of X-ray luminosity densities

In a similar vein, we can also estimate the luminosity densities (as opposed to the cumulative emitted energy densities) at a given redshift as a function of unknown physical parameters. This quantity is more relevant for predicting the X-ray background as a function of redshift.

Suppose that central BHs in galaxies possess an average fraction  $f_{\text{BH}}$  of the dark matter halo mass, and that at any given time they shine at an average fraction  $f_{\text{Edd}}$  (allowing that a fraction of BHs are inactive, and that not all haloes/galaxies host a central BH). Then the 2 – 10 keV luminosity density of active BHs can be written as

$$l_{\text{BH},X} = 1.3 \times 10^{38} f_{\text{bol}} f_{\text{BH}} f_{\text{Edd}} \\ \times \rho_{\text{halo}}(M > M_{\text{host}}) \text{ erg s}^{-1} M_{\odot}^{-1}, \quad (6)$$

where  $1.3 \times 10^{38} \text{ erg s}^{-1} M_{\odot}^{-1}$  is the ratio of the Eddington luminosity of an object to its mass,  $M_{\text{host}}$  is the minimum characteristic mass for a dark matter halo to host a nuclear BH (i.e. the halo mass scale above which the fraction of haloes that host a BH is close to one), and  $\rho_{\text{halo}}(M > M_{\text{host}})$  is the universal density of mass locked in DM haloes above that mass.

The average Eddington ratio  $f_{\text{Edd}}$  (over all haloes with  $M > M_{\text{host}}$ , including those that do not contain an accreting nuclear BH) may be much higher at  $z \gtrsim 6$  than in the local Universe, where it is  $f_{\text{Edd}}(z=0) \ll 1$ . Clustering data suggest that the duty cycle of quasars increases toward high redshift, reaching  $\sim 0.5$  at  $z \approx 5$  (e.g. Shankar, Weinberg & Miralda-Escudé 2009), compared to  $\ll 1$  at  $z \lesssim 2$ . Such prolific activity of high-redshift SMBHs could be explained if their growth is triggered by the major merger rate of galaxies (Li et al. 2007; Tanaka 2014), which scales as  $\sim (1+z)^{5/2}$ .

Turning to the X-ray luminosity from HMXBs, we can write equation (4) as a luminosity density that scales with

the universal star formation rate density,

$$\begin{aligned}
 l_{*,X} &= \ell_X \frac{d}{dt} \rho_{\text{halo}}(M > M_4) \\
 &= \ell_X f_* \frac{\Omega_b}{\Omega_0} \left| \frac{dz}{dt} \right| \zeta(z) \rho_{\text{halo}}(M > M_4) \\
 &\approx 5.7 \times 10^{28} \ell_{X,39} \left( \frac{f_*}{0.1} \right) \left( \frac{1+z}{21} \right)^{5/2} \zeta(z) \\
 &\quad \times \rho_{\text{halo}}(M > M_4) \text{ erg s}^{-1} \text{M}_{\odot}^{-1}.
 \end{aligned} \tag{7}$$

Above,  $\zeta(z) \equiv -d \ln \rho_{\text{halo}}(M > M_4)/dz$  is a dimensionless quantity that is of order unity at redshift values of interest in this paper.

The ratio of the X-ray luminosity density produced by accreting BH seeds to that produced by HMXBs is:

$$\begin{aligned}
 \frac{l_{\text{BH},X}}{l_{*,X}} &\sim 5 \times 10^3 \ell_{X,39}^{-1} f_{\text{Edd}} \left( \frac{f_{\text{BH}}}{10^{-3}} \right) \left( \frac{f_{\text{bol}}}{0.05} \right) \left( \frac{f_*}{0.1} \right)^{-1} \\
 &\quad \times \left( \frac{M_{\text{host}}}{M_4} \right)^{-1} \left( \frac{1+z}{21} \right)^{-5/2} \zeta^{-1}(z).
 \end{aligned} \tag{8}$$

Above, we have used the fact that the DM halo mass function  $dn/dM_{\text{halo}}$  roughly scales as  $M_{\text{halo}}^{-2}$  at masses below the exponential cutoff of the mass function. Once again, we arrive at the conclusion that X-ray emission from growing seed BHs very plausibly dominated over the X-ray emission from HMXBs, *unless* growing nuclear BHs were rare compared to star-forming galaxies, or these BHs emitted much less energy in X-rays per unit mass growth than their present-day counterparts.

It is important to note that the above estimates hold even if only a small fraction of the first PopIII-forming minihaloes formed seed BHs with  $\sim 100 \text{ M}_{\odot}$ . This is because such haloes merge rapidly, and the fraction of haloes containing a seed BH rapidly approaches unity (see e.g. Tanaka & Haiman 2009). For example, a typical halo with a mass  $> 10^{12} \text{ M}_{\odot}$  at  $z \approx 6$  will have had hundreds of thousands to millions of progenitor haloes that formed PopIII stars. Below, we present results from one model that assumes that a X-ray luminous PopIII seed BH forms in all haloes that reach a virial temperature of 2000 K, and another model that assumes that they form in only 1% of such haloes. Both models arrive at approximately the same SMBH population by  $z \approx 6$  (cf. Tanaka & Haiman 2009; Tanaka, Perna & Haiman 2012).

### 3 THEORETICAL MODEL

We summarize our computational scheme as follows.

(i) Using a Monte Carlo merger tree code, we simulate the assembly history of dark matter haloes from  $z \sim 50$  to  $z = 6$ . The algorithm (Zhang, Fakhouri & Ma 2008) and halo sample, which reproduce the Sheth & Tormen (2002) mass function with high fidelity, are the same as those described in Tanaka & Li (2014). We also account for the suppression of PopIII seed formation at high redshifts due to supersonic coherent motions of baryons against dark matter (Tanaka, Li & Haiman 2013, and refs. therein).

(ii) We plant seed BHs in DM haloes that satisfy specific analytic criteria, motivated by the physical models considered. In models with PopIII seed BHs, the seeds are al-

lowed to form when the halo reaches a virial temperature of 2000 K, which is the approximate threshold for PopIII star formation. In models with DCBH seeds, we plant central BHs with masses of  $10^4$ – $10^5 \text{ M}_{\odot}$  in a small fraction of haloes above the atomic-cooling threshold.

(iii) We allow BHs to grow via gas accretion, again following semi-analytic prescriptions following plausible BH-halo scaling relations (motivated by empirical BH-galaxy scaling relations), while also satisfying observational constraints such as the universal SMBH mass density. In our fiducial prescription, BHs accrete to approach a relation  $M_{\text{BH}}(M_{\text{halo}}, z)$  motivated by Ferrarese (2002), at accretion rates capped at the Eddington limit. While we treat the accretion as being continuous, quantitatively similar SMBH populations emerge in models where BH growth occurs sporadically, e.g. triggered by major mergers of the host DM halo (Tanaka, Perna & Haiman 2012; Tanaka 2014). We model the X-ray emission of BHs using standard accretion flow theory, and assume 5 per cent of the emitted energy is reprocessed into a power-law corona with  $E > 1 \text{ keV}$  via Compton upscattering (e.g. Hopkins, Richards & Hernquist 2007; Done et al. 2012). In all models considered in this paper, BH growth and HMXB activity occur only when the host halo is atomic-cooling ( $T_{\text{vir}} > 10^4 \text{ K}$ ).

(iv) We allow the central BHs to merge after their host haloes merge (as long as the halo merger timescale does not exceed the Hubble time, in which case the haloes are assumed to become satellites), and determine semi-analytically whether the merged products are ejected or retained after undergoing gravitational recoil (see Tanaka & Haiman 2009, for details).

(v) Concurrently with the BH growth, we follow the universal star-formation rate and the corresponding X-ray emission from young stellar populations, by assuming that the star formation rate scales with the increase in the baryonic mass content of the halo (see the previous and following sections).

(vi) At each timestep in the merger tree code, we track the cumulative X-ray background for photons with sufficiently long mean-free-paths ( $\gtrsim 1 \text{ keV}$ ) to form an isotropic background. We account for absorption through a neutral IGM, as well as redshifting. We use the time-dependent X-ray background to compute the evolution of the mean IGM kinetic temperature  $T_{\text{IGM}}(z)$ , which in turn is used to give the global (sky-averaged) 21 cm spin temperature. We follow Pritchard & Furlanetto (2006) and Furlanetto & Pritchard (2006) in evaluating the Ly $\alpha$  background and UV emission from stellar populations.

Most of the key model ingredients described above, such as the X-ray output from the first galaxies and the growth of seed BHs, contain large theoretical uncertainties (and are active topics of research in their own right). The goal of this work is not to make specific predictions for every combination of plausible theoretical models, but rather to illustrate the fact that different families of models can correspond to broadly quantitatively distinct predictions for the global 21 cm signature. Whereas previous analyses assumed that the growth of the X-ray background scales directly with the growth in the overall mass density locked inside collapsed dark matter haloes, here we account for relevant effects in the hierarchical SMBH-halo assembly process, such as in-



dividually limiting BH growth to the Eddington limit, occupation fractions and BH-halo scaling relations, as well as BH mergers and the associated gravitational recoil effect.

### 3.1 Global signatures of X-ray emission on the 21cm transition line

Prior to reionization, the thermal history of the IGM is most directly observable using the highly redshifted 21 cm line of neutral hydrogen. The line is globally observable in contrast to the temperature of the CMB with a brightness temperature of

$$T_b^{21\text{ cm}} = 41.5x_H \left(1 - \frac{T_{\text{CMB}}(z)}{T_{21}}\right) \left(\frac{1+z}{21}\right)^{1/2} \text{ mK}, \quad (9)$$

where  $x_H$  is the neutral hydrogen fraction,  $T_{\text{CMB}}(z)$  is the CMB temperature at redshift  $z$ , and  $T_{21}$  is the spin temperature of the neutral hydrogen (see, e.g., Furlanetto 2006, for a more thorough discussion). The 21 cm spin temperature of HI couples to the thermal temperature of the gas mainly through the scattering of Lyman- $\alpha$  photons (Wouthuysen 1952; Field 1958) from the first stars, with

$$T_{21}^{-1} = \frac{T_{\text{CMB}}^{-1} + T_{\text{IGM}}^{-1}(x_\alpha + x_c)}{1 + x_\alpha + x_c}, \quad (10)$$

where  $x_\alpha$  is the coupling coefficient of the 21 cm line to Lyman- $\alpha$  radiation and  $x_c$  is the collisional coupling coefficient, whose contribution is negligible at  $z \lesssim 40$ . Once the star formation rate grows to be  $\gtrsim 10^{-3} M_\odot \text{ yr}^{-1}$ , there are a sufficient number of Lyman- $\alpha$  photons to fully couple the spin temperature to the thermal temperature of the IGM,  $T_{21} \approx T_{\text{IGM}}$  (McQuinn & O’Leary 2012).

We compute the coefficient  $x_\alpha$  following Pritchard & Furlanetto (2006), summing the flux across the Lyman series weighted by “recycling coefficients.” The Lyman- $\alpha$  background is computed by assuming that 9690 photons are produced, per baryon, between Lyman- $\alpha$  and the Lyman limit, with a power-law spectrum  $\varepsilon_\nu \propto \nu^{-0.86}$  (the PopII star spectral model of Barkana & Loeb 2005). We also calculate the dimensionless factor  $S_\alpha$  that goes into computing the coefficient  $x_\alpha$ , following the wing approximation results of Furlanetto & Pritchard (2006; instead of assuming  $S_\alpha = 1$ ).

Generally, the kinetic temperature of the IGM evolves according to

$$\frac{du}{dt} = -p \frac{d}{dt} \left( \frac{1}{\rho} \right) + \frac{\lambda_{\text{net}}}{\rho}, \quad (11)$$

where  $u$ ,  $p$  and  $\rho$  are the mean specific internal energy, pressure and density of the IGM. The first term on the right-hand side, involving the derivative of the IGM density, is dominated by adiabatic cooling due to cosmic expansion. The second term includes line and continuum cooling, as well as Compton heating/cooling. It also includes radiative heating by X-rays, which is the focus of this work. In this work, we calculate radiative transfer and chemistry for the species H,  $\text{H}^+$ , He,  $\text{He}^+$  and  $\text{He}^{++}$ . We refer the reader to Tanaka, Perna & Haiman (2012) for further details.

In a neutral IGM, photons with energies above  $\approx 1$  keV have mean free paths longer than the Hubble horizon, and will build up an X-ray background that isotropically heats the IGM. We assume that the primary astrophysical sources

of X-rays are young stellar populations and (mini-) quasars, i.e. SMBHs (or their progenitors) that are undergoing luminous accretion. Below, we describe our theoretical treatment of each of type of X-ray source.

### 3.2 X-ray Sources

#### 3.2.1 Stellar populations (HMXBs)

Following Furlanetto (2006), we assume that the global  $> 1$  keV X-ray emission from high-redshift galaxies is proportional to the star formation rate (as is observed for local star-forming galaxies; see §2), and that as DM haloes grow in mass, they convert a fraction  $f_* \sim 0.1$  of their baryons into stars.<sup>2</sup>

Following eq. 2, the luminosity density in  $2 - 10$  keV X-rays produced by star formation in the early Universe at any redshift can be estimated as

$$\epsilon_{2-10 \text{ keV}} = \ell_{X,*} \rho_* = \ell_{X,*} f_* \frac{d}{dt} \rho_{\text{halo}}(M > M_4), \quad (12)$$

where  $\rho_{\text{halo}}(M > M_4)$  is the density of matter locked inside haloes above the atomic-cooling threshold. We assume that the spectral energy distribution from young stellar populations takes the form of a power-law in the relevant energy range (i.e. hard enough to form a background), with index  $\Gamma = 1.8$  (e.g. Swartz et al. 2004); equation (12) gives the normalization to this power-law.

As stated in 3, we only allow HMXBs and seed BH growth in haloes with  $T_{\text{vir}} > 10^4$  K. This is a conservative prescription, based on the simple fact that ionization resulting from mini-quasar activity can unbind the gas from haloes with shallower potentials (see also Alvarez, Wise & Abel 2009; Milosavljević et al. 2009; Park & Ricotti 2012, for additional possible consequences of radiative feedback).

In principle, haloes in the range  $2000 \text{ K} \lesssim T_{\text{vir}} \lesssim 10^4 \text{ K}$  could also produce X-rays via nuclear BH growth or HMXB activity. Such a scenario would result in additional heating as early as  $z \approx 30$ , with a corresponding turn in the 21 cm signature.

It is uncertain whether the quantity  $\ell_{X,*}$ , which has been measured to be  $\gtrsim 10^{39} \text{ ergs}^{-1} M_\odot^{-1} \text{ yr}$  in star-forming galaxies in the local Universe (e.g. Glover & Brand 2003; Mineo, Gilfanov & Sunyaev 2012), evolves with redshift. Following Dijkstra et al. (2012), we parameterize this uncertainty by adopting a functional form

$$\ell_{X,*}(z) = \ell_{X,*}(z=0) \times (1+z)^b. \quad (13)$$

We adopt  $\ell_{X,*}(z=0) = 3 \times 10^{39} \text{ ergs}^{-1} M_\odot^{-1} \text{ yr}$ , and consider two extreme cases for the parameter  $b$ : (i) a conservative case  $b = 0$  (i.e. no redshift evolution), and (ii) a more prolific case  $b = 1$ , which is consistent with observations out to  $z \approx 4$  (Basu-Zych et al. 2013), but lies near the  $1 - \sigma$  exclusion limit for higher redshifts (Dijkstra et al. 2012).

<sup>2</sup> Although we consider HMXBs as the chief emitter of X-rays from stellar populations, other sources, such as supernova remnants, could also contribute. However, such sources can be incorporated into the quantity  $\ell_X$  (X-ray emission per star formation rate), as long as they are associated with young stars.

### 3.2.2 Seed BHs

We consider both PopIII and DCBH seed models.

For the PopIII case, we assume that seed BHs can form once a dark matter halo reaches a virial temperature of 2000 K, which is roughly the threshold required for molecular hydrogen to form, leading to PopIII star formation. Once a DM halo reaches this virial temperature, a seed BH forms in the mass range  $10 M_{\odot} < M < 300 M_{\odot}$  with a mass function and power-law slope  $-1.35$ , excluding the pair-instability window of  $140 - 260 M_{\odot}$ . While the mass distribution of PopIII stars remains a topic of active research (Hirano et al. 2014, 2015), we believe our choice of a steep power-law is conservative as only a small fraction of haloes form seed BHs with masses  $\gtrsim 100 M_{\odot}$ . We consider a case where a PopIII seed BH forms in each halo reaching  $T_{\text{vir}} = 2000$  K, and another in which a seed BH forms in only 1 per cent of such haloes.

For the DCBH case, we assume that a seed BH with a mass of  $10^5 M_{\odot}$  forms in a small fraction of haloes reaching the atomic-cooling threshold of  $T_{\text{vir}} = 10^4$  K.

This corresponds to a scenario in which pristine atomic-cooling haloes are irradiated by UV light from nearby star-forming galaxies, thereby suppressing ordinary PopIII star formation via photodissociation of  $\text{H}_2$  molecules. Under such conditions, the gas can only cool via atomic cooling transitions, and collapses isothermally at a temperature  $\sim 10^4$  K, forming a so-called “supermassive” ( $\sim 10^5 M_{\odot}$ ) star that leaves behind a BH of similar mass via general-relativistic instability. While the exact conditions necessary for this mode of BH formation, and how often they occur in nature, remain uncertain, recent theoretical estimates suggest that DCBH formation may be able to explain the abundance of the most luminous  $z \sim 6$  quasar SMBHs (comoving number density of  $\sim 1 \text{ Gpc}^{-3}$  at  $z \approx 6$ ) but not the general SMBH population (Dijkstra, Ferrara & Mesinger 2014; Latif et al. 2015; Inayoshi & Tanaka 2014).

We consider a somewhat generous DCBH-seeding prescription, in which 0.01 per cent ( $10^{-4}$ ) of all haloes reaching the atomic-cooling threshold within a redshift range  $20 > z > 10$  form a DCBH of mass  $10^5 M_{\odot}$ . This seeding prescription is sufficient to ensure that most galaxy-class haloes host a SMBH by  $z \approx 6$  and at later epochs.

### 3.3 Limitations

In this work, we focus on the initial turnover feature of the global 21 cm signature. We do not follow the signature past  $z \approx 12$ , for the following two reasons.

First, our computational algorithm tracks the mean thermal evolution of the IGM due to an isotropic X-ray background. Because the code does not track the spatial distribution of the dark matter haloes, we cannot follow the localized, expanding ionized regions that form around individual star-forming galaxies and quasars due to their UV emission (whereas  $> 1$  keV X-rays propagate for  $\sim 1$  Gpc before being absorbed). The strength of the 21 cm signature depends on the column density of neutral hydrogen in the IGM; because our computational method cannot reliably track the latter quantity in an anisotropically ionized Universe, we refrain from modeling the signature into the epoch of UV-driven reionization, i.e.  $z \lesssim 12$ .

Second, it is plausible that the heating of the IGM affects star formation and (mini-) quasar activity in low-mass galaxies (Ripamonti, Mapelli & Zaroubi 2008; Tanaka, Perna & Haiman 2012). Once the IGM temperature rises, gas infall into galaxies that fall below the Jeans collapse scale (or the filtering mass scale; e.g. Gnedin 2000; Naoz & Barkana 2007) may be suppressed, quenching star formation and (mini-) quasar activity in these sites. As a reference, the Jeans mass scale becomes larger than the atomic-cooling halo virial mass threshold at  $T_{\text{IGM}} \sim 10^3$  K. Because there are numerous uncertainties regarding the details of this global, thermally driven feedback, we do not attempt to model the regime where it becomes important.

In other words, the initial rise in the global 21 cm signature at  $20 \lesssim z \lesssim 30$  depends only on the heating rate of the IGM during this epoch, whereas the signature at later times depends on the progress of reionization, as well as how effectively gas from a heated IGM can collapse into low-mass haloes. We concentrate on the former signature.

## 4 RESULTS

### 4.1 IGM kinetic temperature

In Figure 1, we show the redshift evolution of the mean IGM kinetic temperature. We will describe the curves in order, roughly from bottom to top, as follows. The solid black line at the very bottom shows, for reference, the null case with adiabatic cooling due to cosmic expansion and no heat sources.

With the exception of the adiabatic case, all of the models include X-ray heating from HMXBs. In models with thin lines, it’s assumed that the factor  $\ell_{\text{X},*}$  (which relates X-ray production to star formation rate) is the same as measured in star-forming galaxies the local-Universe; in those with thick lines, this quantity increases toward high redshift as  $\ell_{\text{X},*} \propto (1+z)$ .

The thin, magenta line and the thick, red line (both dotted) show cases where HMXBs are the only X-ray sources heating the IGM. The former, which assumes that X-ray production per star formation rate (the quantity  $\ell_{\text{X},*}$ ) does not evolve with redshift, results in the IGM kinetic temperature increasing at  $z \sim 20$ . For the latter case, which assumes that  $\ell_{\text{X},*} \propto (1+z)$ ,  $T_{\text{IGM}}$  increases at  $z \sim 25$ .

The thick, green curve and the thin, dark green curve (both long-dashed) show models where DCBHs with  $M = 10^5 M_{\odot}$  form in 0.01% of atomic-cooling haloes at  $z < 15$ , and grow to match the prescribed relationship  $M_{\text{BH}}(M_{\text{halo}}, z)$ , with accretion capped at the Eddington rate. Note that this seeding fraction of 0.01% is much larger than found in recent theoretical work, which suggest that DCBHs may have challenges in matching the observed abundance of high-redshift quasars (Dijkstra, Ferrara & Mesinger 2014; Latif et al. 2015; Inayoshi & Tanaka 2014). These heating curves are the same as HMXB-only cases described in the previous paragraph, except for the additional heating at late times ( $z \lesssim 15$ ) due to the emergence of DCBH seeds.

Finally, the blue and cyan lines (both thick and short-dashed) show cases in which a PopIII seed BH forms in haloes reaching virial temperatures  $T_{\text{vir}} = 2000$  K, and

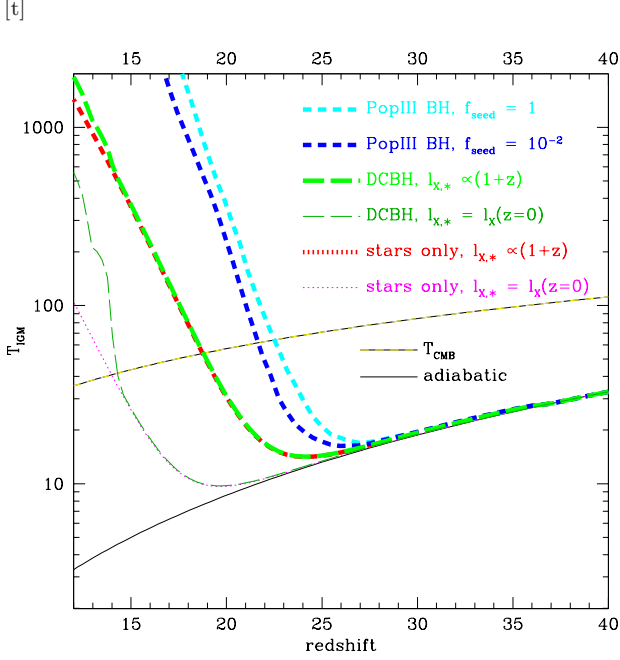


**Figure 1.** The IGM temperature (as contrasted to pure adiabatic cooling) resulting from different sources of heating: direct collapse BHs (green and dark green lines) and BHs from PopIII seeds (blue and cyan lines), both including the contribution from HMXBs. The effect of HMXBs alone is also displayed separately (magenta and red lines). Two prescriptions (compatible with independent constraints) are considered for each heating source. Heating from PopIII BHs dominates over that of HMXBs alone, while the contribution from DCBHs is comparable or subdominant with respect to that of HMXBs, until  $z \approx 15$ . For reference, we have also plotted what the IGM temperature would be with adiabatic cooling alone (solid black curve), as well as the CMB temperature (which determines when the 21 cm line goes into emission; yellow-and-black dashed curve).

promptly begins to accrete gas as the host halo also grows. The cyan line shows the case where such a growing seed forms in all  $T_{\text{vir}} > 2000$  K haloes, and the blue line shows the case where a seed forms in 1 per cent of such haloes. Both cases assume an HMXB contribution  $\ell_{X,*} \propto (1+z)$ , but it is clear that the mini-quasar activity of PopIII BHs dominate.

The PopIII seed models heat the IGM much earlier than models that include HMXB heating only (which, again, use the growth in  $\rho_{\text{halo}}(M > M_4)$  as a proxy for star-formation; Furlanetto 2006). Again, the former assumes that seed BHs form in  $> 1\%$  of  $T_{\text{vir}} \approx 2000$  K haloes, and grow to match extrapolated BH-halo scaling relations in all haloes with  $T_{\text{vir}} > 10^4$  K.

It is important to point out that even if PopIII remnants produce copious X-rays, they may not contribute significantly to the present-day X-ray background. This is because their spectra are expected to be relatively soft, as well as sharply peaked in intrinsic X-rays. For example, a blackbody, Eddington-rate accretion disc around a  $10^3 M_{\odot}$  BH has a spectrum that peaks at  $\approx 0.3$  keV and drops off by orders of magnitude above  $\approx 1$  keV. A graybody disc (Blaes 2004; Tanaka & Menou 2010) can be harder and peak at  $\approx 1$  keV. In either case, the bulk of the emission would

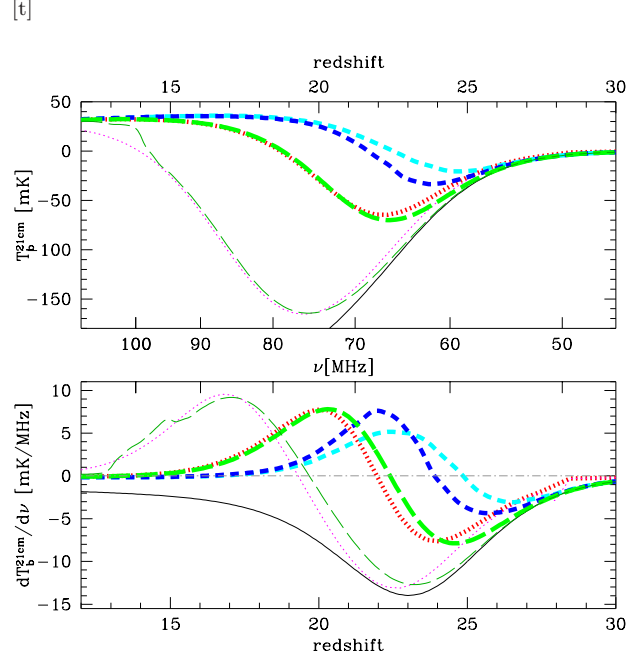


**Figure 2.** The brightness temperature of the 21 cm radiation (top panel), and its spectrum (bottom panel) for a medium heated by HMXBs alone, or with the inclusion of accreting BHs either in the DCBH scenario or in the PopIII formation scenario. Line types and colors refer to the same models as in Fig. 1.

be redshifted to energies well below the  $\approx 0.1$  keV limit of soft X-ray observatories. Therefore, it is plausible that the vast majority of the X-rays emitted by miniquasars at  $z \gtrsim 20$  is redshifted into the FUV, and be minimally reflected in the present-day X-ray background. Note the contrast to present-day AGN, whose intrinsic spectra peak in the UV and whose X-ray emission consists of a power-law tail (cf. Salvaterra et al. 2012, who consider limits on early SMBH growth by assuming power-law X-ray spectra).

#### 4.2 21 cm brightness temperature

After the first stars form, the thermal history of the IGM is directly imprinted in the 21 cm brightness temperature. One of the most important characteristics of the global, sky-averaged 21 cm signal is when it reaches its minimum. This turning point occurs when the IGM transitions from primarily adiabatic cooling to the epoch of heating (Furlanetto 2006; Pritchard & Loeb 2008; Mirocha, Harker & Burns 2013), which is sensitive to the accretion history of the first black holes. A number of experiments have been proposed, or are currently underway, to detect this signal—e.g. the Dark Ages Radio Explorer<sup>3</sup> (DARE; Burns et al. 2012), the Large-Aperture Experiment to Detect the Dark Ages<sup>4</sup> (LEDA), the Experiment to Detect the Global EoR Step (EDGES; Bowman, Rogers & Hewitt 2008), and SCI-HI (Voytek et al. 2014).

<sup>3</sup> <http://lunar.colorado.edu/dare/>

<sup>4</sup> <https://www.cfa.harvard.edu/LEDA/>

The upper panel of Figure 2 shows the 21 cm brightness temperature  $T_b^{21\text{cm}}$  as a function of redshift for the same models shown in Figure 1. These models use the same line styles and follow the same order as discussed in § 4.1. Because PopIII BH models rapidly accrete gas, they begin heating the IGM as soon as they form. The total amount of X-ray heating dominates over stellar sources (HMXBs and supernova remnants). As a result, our PopIII BH models increase in brightness temperature beginning at  $z \lesssim 25$ , at typically  $\approx 20$  mK above the adiabatic case. The detection of such a signature would strongly suggest either (i) stellar populations from the earliest galaxies produced far more X-rays per unit mass formed in stars than what is observed from nearby star-forming galaxies, or (ii) nuclear BHs were prolifically emitting X-rays as mini-AGN at these redshifts (much earlier than predicted by most DCBH scenarios).

In contrast to the PopIII models, the DCBH models do not produce sufficient X-rays to significantly heat the IGM before  $z \gtrsim 20$ . HMXBs produced in ordinary stellar evolution dominate the IGM heating while the 21 cm signal is in absorption. Because the gas has more time to adiabatically cool, the resulting signal is intrinsically stronger and easier to detect with a lower foreground sky temperature (Furlanetto, Oh & Briggs 2006). If the 21 cm trough is detected at late times, either the PopIII BHs were heavily obscured, or the BHs that are the progenitors of SMBHs formed via direct collapse.

At the frequencies required to detect the dark ages (50–90 MHz) the observations will be dominated by *smooth* Galactic foreground emission. The 21 cm signal contributes only about 1 part in  $10^4$  to the total signal. The 21 cm signal is detectable by the variations of the brightness temperature with frequency. The lower panel of figure 2 shows the derivative of the brightness temperature,  $dT_b^{21\text{cm}}/d\nu$ , as a function of  $z$ , for the same models.

An upward trend in the 21 cm brightness temperature prior to  $z \gtrsim 20$  strongly implies rampant PopIII seed growth, or a much higher X-ray production from young stellar populations than seen in the local Universe. At these frequencies, planned experiments are dominated by systematic uncertainties. For example, DARE will have a measurement uncertainty of order 1 mK at these frequencies after 3000 h of integration. In addition, it is capable of determining when the brightness temperature reaches a minimum to  $\delta z \approx 0.4$ . Typical uncertainties in the minimum temperature are expected to be  $\delta T_b^{21\text{cm}}/T_b^{21\text{cm}} \approx 15\%$  for models similar to the ones considered here (Harker et al. 2012).

Finally, more stringent constraints on the progenitors of SMBHs may be made by combining the global 21 cm observations with other techniques. For example, observations of the evolution of star formation at high redshift may be able to constrain the contribution of stellar sources to the IGM heating. Angular correlations in the 21 cm signal (Pritchard & Loeb 2008; McQuinn & O’Leary 2012; Visbal et al. 2012) may also be able to ascertain the characteristic dark matter halo masses that dominate the IGM heating.

Both reionization and thermal feedback on baryonic structure formation would suppress the 21 cm brightness temperature at late times. An upward trend in the brightness temperature at  $z \lesssim 15$  would therefore strongly imply that SMBH growth began in earnest at this epoch.

## 5 SUMMARY

IGM heating by the first radiation sources leaves a marked imprint on the 21 cm radiation. Here, using both analytical arguments as well as Monte Carlo simulations, we have argued that the primary driver of IGM heating are the BH remnants of PopIII stars, if these are the progenitors of the SMBHs observed in the Universe. In this scenario, heating by these sources would dominate over the other main contribution, i.e. HMXBs, unlike the case in which SMBHs grow from DCBHs, which we find to be subdominant with respect to HMXBs.

Our work in estimating the 21 cm signature of the progenitors of SMBHs is distinct in three respects. First, the total BH mass density in our models does not grow in proportion to the total mass density locked inside dark matter haloes (as in most previous works, e.g. Furlanetto 2006; Pritchard & Loeb 2008; Mirocha 2014), but are grown individually while reflecting effects such as the Eddington accretion limit, mergers, and gravitational recoil. Second, we explicitly treat the propagation and absorption of the X-rays averaged over the cosmological volume (Mirocha 2014). Finally, our models are constrained to those that reproduce the properties of high redshift quasars (Tanaka, Perna & Haiman 2012; Tanaka, Li & Haiman 2013).

The 21 cm signal, with its sensitivity to the heating history of the Universe, hence becomes a powerful tool to probe the progenitors of SMBHs, and their growth history. In particular, we have shown that a trend upward in the brightness temperature of the 21 cm radiation would indicate an abundant production of PopIII seed BHs, and hence would lend support to a scenario in which the growth of the SMBHs originated from those.

## ACKNOWLEDGMENTS

We thank the reviewer, Emanuele Ripamonti, for constructive comments that helped improve the clarity of the manuscript.

## REFERENCES

- Abel T., Bryan G. L., Norman M. L., 2002, *Science*, 295, 93
- Aller M. C., Richstone D., 2002, *AJ*, 124, 3035
- Alvarez M. A., Wise J. H., Abel T., 2009, *ApJ*, 701, L133
- Barkana R., Loeb A., 2005, *ApJ*, 626, 1
- Barth A. J., Ho L. C., Rutledge R. E., Sargent W. L. W., 2004, *ApJ*, 607, 90
- Basu-Zych A. R. et al., 2013, *ApJ*, 762, 45
- Begelman M. C., Volonteri M., Rees M. J., 2006, *MNRAS*, 370, 289
- Blaes O. M., 2004, in *Accretion Discs, Jets and High Energy Phenomena in Astrophysics*, V. Beskin, G. Henri, F. Menard, G. Pelletier, J. Dalibard, ed., Springer Publishing Company, New York, NY, USA, pp. 137–185
- Bowman J. D., Rogers A. E. E., Hewitt J. N., 2008, *ApJ*, 676, 1
- Bromm V., Coppi P. S., Larson R. B., 2002, *ApJ*, 564, 23
- Bromm V., Loeb A., 2003, *ApJ*, 596, 34



- Burns J. O. et al., 2012, *Advances in Space Research*, 49, 433
- Cattaneo A. et al., 2009, *Nature*, 460, 213
- Dijkstra M., Ferrara A., Mesinger A., 2014, *ArXiv e-prints* 1405.6743
- Dijkstra M., Gilfanov M., Loeb A., Sunyaev R., 2012, *MNRAS*, 421, 213
- Done C., Davis S. W., Jin C., Blaes O., Ward M., 2012, *MNRAS*, 420, 1848
- Fan X. et al., 2001, *AJ*, 122, 2833
- Fender R., Belloni T., 2012, *Science*, 337, 540
- Ferrarese L., 2002, *ApJ*, 578, 90
- Field G. B., 1958, *Proceedings of the IRE*, 46, 240
- Fragos T. et al., 2013a, *ApJ*, 764, 41
- Fragos T., Lehmer B. D., Naoz S., Zezas A., Basu-Zych A., 2013b, *ApJ*, 776, L31
- Fukugita M., Peebles P. J. E., 2004, *ApJ*, 616, 643
- Furlanetto S. R., 2006, *MNRAS*, 371, 867
- Furlanetto S. R., Oh S. P., Briggs F. H., 2006, *Phys. Reports*, 433, 181
- Furlanetto S. R., Pritchard J. R., 2006, *MNRAS*, 372, 1093
- Glover S. C. O., Brand P. W. J. L., 2003, *MNRAS*, 340, 210
- Gnedin N. Y., 2000, *ApJ*, 542, 535
- Greif T. H., Springel V., White S. D. M., Glover S. C. O., Clark P. C., Smith R. J., Klessen R. S., Bromm V., 2011, *ApJ*, 737, 75
- Grimm H.-J., Gilfanov M., Sunyaev R., 2003, *MNRAS*, 339, 793
- Haiman Z., 2013, in *Astrophysics and Space Science Library*, Vol. 396, *Astrophysics and Space Science Library*, Wiklund T., Mobasher B., Bromm V., eds., p. 293
- Haiman Z., Loeb A., 2001, *ApJ*, 552, 459
- Harker G. J. A., Pritchard J. R., Burns J. O., Bowman J. D., 2012, *MNRAS*, 419, 1070
- Hirano S., Hosokawa T., Yoshida N., Omukai K., Yorke H. W., 2015, *MNRAS*, 448, 568
- Hirano S., Hosokawa T., Yoshida N., Umeda H., Omukai K., Chiaki G., Yorke H. W., 2014, *ApJ*, 781, 60
- Ho L. C., Filippenko A. V., Sargent W. L. W., Peng C. Y., 1997, *ApJS*, 112, 391
- Hopkins P. F., Richards G. T., Hernquist L., 2007, *ApJ*, 654, 731
- Hummel J. A., Stacy A., Jeon M., Oliveri A., Bromm V., 2014, *ArXiv e-prints*
- Inayoshi K., Tanaka T. L., 2014, *ArXiv e-prints*
- Islam R. R., Taylor J. E., Silk J., 2003, *MNRAS*, 340, 647
- Izotov Y. I., Thuan T. X., 2008, *ApJ*, 687, 133
- Kormendy J., Ho L. C., 2013, *ARAA*, 51, 511
- Koushiappas S. M., Bullock J. S., Dekel A., 2004, *MNRAS*, 354, 292
- Latif M. A., Bovino S., Grassi T., Schleicher D. R. G., Spaans M., 2015, *MNRAS*, 446, 3163
- Li Y. et al., 2007, *ApJ*, 665, 187
- Lodato G., Natarajan P., 2006, *MNRAS*, 371, 1813
- Madau P., Haardt F., Dotti M., 2014, *ApJ*, 784, L38
- Madau P., Rees M. J., 2001, *ApJ*, 551, L27
- Marconi A., Risaliti G., Gilli R., Hunt L. K., Maiolino R., Salvati M., 2004, *MNRAS*, 351, 169
- McQuinn M., O’Leary R. M., 2012, *ApJ*, 760, 3
- Micic M., Holley-Bockelmann K., Sigurdsson S., 2011, *MNRAS*, 414, 1127
- Milosavljević M., Bromm V., Couch S. M., Oh S. P., 2009, *ApJ*, 698, 766
- Mineo S., Gilfanov M., Lehmer B. D., Morrison G. E., Sunyaev R., 2014, *MNRAS*, 437, 1698
- Mineo S., Gilfanov M., Sunyaev R., 2012, *MNRAS*, 419, 2095
- Mirocha J., 2014, *ArXiv e-prints*
- Mirocha J., Harker G. J. A., Burns J. O., 2013, *ApJ*, 777, 118
- Mortlock D. J. et al., 2011, *Nature*, 474, 616
- Naoz S., Barkana R., 2007, *MNRAS*, 377, 667
- O’Leary R. M., Loeb A., 2009, *MNRAS*, 395, 781
- Park K., Ricotti M., 2012, *ApJ*, 747, 9
- Pritchard J. R., Furlanetto S. R., 2006, *MNRAS*, 367, 1057
- Pritchard J. R., Loeb A., 2008, *PRD*, 78, 103511
- Rashkov V., Madau P., 2014, *ApJ*, 780, 187
- Reines A. E., Greene J. E., Geha M., 2013, *ApJ*, 775, 116
- Ricotti M., Ostriker J. P., 2004, *MNRAS*, 352, 547
- Ricotti M., Ostriker J. P., Gnedin N. Y., 2005, *MNRAS*, 357, 207
- Ripamonti E., Mapelli M., Zaroubi S., 2008, *MNRAS*, 387, 158
- Ryu T., Tanaka T. L., Perna, R., 2015, *arXiv e-prints*
- Salvaterra R., Haardt F., Volonteri M., Moretti A., 2012, *A&A*, 545, L6
- Shakura N. I., Sunyaev R. A., 1973, *A&A*, 24, 337
- Shankar F., Crocce M., Miralda-Escudé J., Fosalba P., Weinberg D. H., 2010, *ApJ*, 718, 231
- Shankar F., Salucci P., Granato G. L., De Zotti G., Danese L., 2004, *MNRAS*, 354, 1020
- Shankar F., Weinberg D. H., Miralda-Escudé J., 2009, *ApJ*, 690, 20
- Sheth R. K., Tormen G., 2002, *MNRAS*, 329, 61
- Soltan A., 1982, *MNRAS*, 200, 115
- Stacy A., Greif T. H., Bromm V., 2010, *MNRAS*, 403, 45
- Swartz D. A., Ghosh K. K., Tennant A. F., Wu K., 2004, *ApJS*, 154, 519
- Tanaka T., Haiman Z., 2009, *ApJ*, 696, 1798
- Tanaka T., Menou K., 2010, *ApJ*, 714, 404
- Tanaka T., Perna R., Haiman Z., 2012, *MNRAS*, 425, 2974
- Tanaka T. L., 2014, *ArXiv e-prints*: 1406.3023
- Tanaka T. L., Li M., 2014, *MNRAS*, 439, 1092
- Tanaka T. L., Li M., Haiman Z., 2013, *MNRAS*, 435, 3559
- Venemans B. P. et al., 2013, *ApJ*, 779, 24
- Visbal E., Barkana R., Fialkov A., Tseliakhovich D., Hirata C. M., 2012, *Nature*, 487, 70
- Volonteri M., 2010, *A&A*, 18, 279
- Volonteri M., Rees M. J., 2005, *ApJ*, 633, 624
- Volonteri M., Silk J., Dubus G., 2015, *ApJ*, 804, 148
- Voytek T. C., Natarajan A., Jáuregui García J. M., Peterson J. B., López-Cruz O., 2014, *ApJ*, 782, L9
- Willott C. J. et al., 2010, *AJ*, 139, 906
- Willott C. J., McLure R. J., Jarvis M. J., 2003, *ApJ*, 587, L15
- Wouthuysen S. A., 1952, *AJ*, 57, 31
- Yajima H., Khochfar S., 2014, *ArXiv e-prints*
- Yoshida N., Omukai K., Hernquist L., 2008, *Science*, 321, 669
- Yu Q., Tremaine S., 2002, *MNRAS*, 335, 965
- Zhang J., Fakhouri O., Ma C., 2008, *MNRAS*, 389, 1521